Am J Physiol Renal Physiol 297: F1288–F1298, 2009.
First published September 2, 2009; doi:10.1152/ajprenal.00388.2009.

Early monitoring of acute tubular necrosis in the rat kidney by ^{23}Na-MRI

Bharath K. Atthe,[1,2] Andriy M. Babsky,[1] Paige N. Hopewell,[1,5] Carrie L. Phillips,[3] Bruce A. Molitoris,[4] and Navin Bansal[1,2,5]

[1]*Departments of Radiology,* [2]*Biomedical Engineering,* [3]*Pathology and Laboratory Medicine, and* [4]*Medicine, Indiana University-Purdue University at Indianapolis, Indianapolis; and* [5]*Weldon School of Biomedical Engineering, Purdue University, West Lafayette, Indiana*

Submitted 9 July 2009; accepted in final form 18 August 2009

Atthe BK, Babsky AM, Hopewell PN, Phillips CL, Molitoris BA, Bansal N. Early monitoring of acute tubular necrosis in the rat kidney by ^{23}Na-MRI. *Am J Physiol Renal Physiol* 297: F1288–F1298, 2009. First published September 2, 2009; doi:10.1152/ajprenal.00388.2009.—Reabsorption of water and other molecules is dependent on the corticomedullary sodium concentration gradient in the kidney. During the early course of acute tubular necrosis (ATN), this gradient is altered. Therefore, ^{23}Na magnetic resonance imaging (MRI) was used to study the alterations in renal sodium distribution in the rat kidney during ischemia and reperfusion (IR) injury, which induces ATN. In-magnet ischemia was induced for 0 (control), 10, 20, 30 or 50 min in Wistar rats. ^{23}Na images were collected every 10 min during baseline, ischemia, and 60-min reperfusion periods. T_1 and T_2 relaxation times were measured by both ^{23}Na-MRI and -MRS on a separate cohort of animals during ischemia and reperfusion for correction of relaxation-related tissue sodium concentration (TSC). A marked decrease was observed in the medulla and cortex ^{23}Na-MRI signal intensity (SI) during the early evolution of ATN caused by IR injury, with the sodium reabsorption function of the kidney being irreversibly damaged after 50 min of ischemia. Sodium relaxation time characteristics were similar in the medulla and cortex of normal kidney, but significantly decreased with IR. The changes in relaxation times in both compartments were identical; thus the medulla-to-cortex sodium SI ratio represents the TSC ratio of both compartments. The extent of IR damage observed with histological examination correlated with the ^{23}Na-MRI data. ^{23}Na-MRI has great potential for noninvasive, clinical diagnosis of evolving ATN in the setup of acute renal failure and in differentiating ATN from other causes of renal failure where tubular function is maintained.

ischemia-reperfusion injury; relaxation times; tissue; sodium concentration

THE KIDNEY MAINTAINS THE HOMEOSTASIS of body fluids and electrolytes using urinary concentration and countercurrent mechanisms. Concentration of the urine requires establishment and maintenance of a hypertonic medullary interstitium (21, 31). The thick ascending limb (TAL) of the loops of Henle power the countercurrent multiplier process responsible for generation of a corticomedullary osmolality gradient (39). The gradient is maintained by the coordinated function of the loops of Henle, the collecting ducts, and the vasa recta (39). A declining corticomedullary osmolality gradient may serve as a very early sign of disruption of the tubular reabsorption function in acute renal failure (ARF) (27).

The two major causes of ARF developing in the hospital are prerenal disease and acute tubular necrosis (ATN). Together, they account for ~70–75% of all causes of ARF. Ischemia remains the major cause of ATN in the adult population. Kidneys injured by ischemia and reperfusion manifest a variety of functional defects, prominent among which is an impairment of tubular reabsorption of sodium and water (29, 38, 40). Clinically, the glomerular filtration rate (GFR) and fractional excretion of sodium (FE_{Na}) are used to assess ATN. The reduction in GFR that occurs in ATN results from hypoperfusion and from casts and debris obstructing tubule lumen, causing backleak of filtrate through the damaged epithelium. Thus GFR is not a direct measure of tubular dysfunction. FE_{Na} is evaluated from the creatinine and sodium concentrations in urine and plasma and has been suggested to differentiate between prerenal disease and ATN. A value $<1\%$ suggests prerenal disease, while a value $>2\%$ usually indicates ATN. A basic disadvantage of urine and blood analysis is that they rely on global measurements and they measure combined functions of both the kidneys. If one kidney is able to compensate for the dysfunction of the other kidney, then the analysis shows normal values. Another challenge is that sodium and creatinine concentrations change significantly only after substantial kidney injury occurs, and then with a time delay. Thus FE_{Na} is not a reliable indicator for the diagnosis of ATN and for predicting or monitoring therapeutic responses. Noninvasive imaging studies have the potential to evaluate the regional function of each kidney separately and provide more reliable functional and metabolic information than is available from blood and/or urine tests.

Sodium-23 (^{23}Na) magnetic resonance imaging (MRI) may be useful in the diagnosis of renal diseases, as sodium plays a major role in fluid and electrolyte homeostasis regulated by the extracellular corticomedullary sodium concentration gradient. A number of studies have demonstrated the value of ^{23}Na-MRI for nondestructively monitoring two- and three-dimensional intrarenal sodium distribution in vivo (3, 11, 24–28, 33, 36, 41). Maril et al. (26) showed for the first time the capability to quantify the sodium gradient in the kidney during loop diuresis, hydroneprhosis, and obstruction of the ureter (25, 27). They also illustrated that the early evolution of nephrotoxic ATN induced by radiological contrast medium manifests with the development of an altered corticomedullary sodium gradient (27), detected noninvasively by ^{23}Na-MRI. Recently, Maril et al. (28) demonstrated the feasibility of using ^{23}Na-MRI to detect the spatial distribution of sodium in human kidney noninvasively.

Herein, ^{23}Na-MRI was applied to study the alterations in renal sodium distribution in the rat kidney during ischemia and reperfusion (IR) injury. Effects of 10-, 20-, 30-, and 50-min ischemia followed by reperfusion were examined to evaluate whether ^{23}Na-MRI can distinguish between reversible and irreversible ischemic tissue damage. ^{23}Na-MRI and -MRS

Address for reprint requests and other correspondence: N. Bansal, Dept. of Radiology, Indiana Univ. School of Medicine, 950 West Walnut St., R2 E124, Indianapolis, IN 46202-5181 (e-mail: nbansal@iupui.edu).

were also applied to evaluate the effects of 50-min ischemia and reperfusion on ^{23}Na relaxation times (T_1 and T_2). These relaxation times were used to quantitatively measure tissue sodium concentrations (TSC) from MRI signal intensity (SI).

MATERIALS AND METHODS

Animal Preparation

All animal studies were approved by the Indiana University Institutional Animal Care and Use Committee. The study was performed using adult male Wistar rats (200–250 g, Harlan, Indianapolis, IN) with free access to food (standard chow diet) and water. The animals were anesthetized with 2% isoflurane delivered in medical air at 2 l/min using a nose mask connected to a gas anesthesia machine (Vetland, Louisville, KY). The abdomen was shaved with clippers and washed with germicidal soap. Animals were placed on a sterile disposable absorbent towel over a warming pad. After ensuring appropriate depth of anesthesia the abdomen was opened by making a 3-cm midline incision. The fat and connective tissue surrounding the left renal artery and vein were dissected away. A 3-0 silk suture (Sofsilk, US Surgical, Norwalk, CT) was placed around the renal artery and vein of the left kidney using a traumatic needle. The ends of the thread were passed through 1-m long and 1/8-in.-diameter fluorinated ethylene propylene plastic tubing (Cole-Parmer, Vernon Hill, IL) to form a snare. The abdominal muscle and skin layers were closed separately with 3-0 silk suture. The snare was used to induce in-magnet ischemia for 0 (control), 10, 20, 30, or 50 min in different groups of rats (n = 5/group) by pulling the snare taut and clamping it in position. For reperfusion, the snare was released with the ligature left loose on the surface of the renal vascular pedicle.

MRI Experiments

All in vivo MRI experiments were performed using a Varian 9.4-T, 31-cm horizontal bore system (Varian, Palo Alto, CA) equipped with a 12-cm gradient insert (maximum gradient strength = 38 G/cm). A loop-gap volume resonator (diameter = 50 mm, depth = 30 mm) tunable to 105 MHz for ^{23}Na and 400 MHz for ^{1}H was used. The anesthesia was maintained with 1.0–1.5% isoflurane delivered in medical air at 1.5–2.0 l/min during the MRI experiments. Warm air was blown through the magnet bore to maintain the animal core temperature at 35–37°C, which was monitored with a rectal fiber-optic probe (FISO Technologies, Quebec, ON). The rat's respiration was monitored using a MR-compatible small-animal monitoring and gating system (SA Instruments, Stony Brook, NY). The animal was placed in the coil, positioned on a custom-designed plastic cradle with the kidney approximately centered in the coil. A detachable cylindrical phantom (diameter = 10 mm, length = 80 mm) consisting of 51.3 mM NaCl was placed inside the resonator near the animal back to serve as the sodium standard. The magnet was shimmed to less than 100 Hz full-width at half-height of the ^{23}Na signal.

^{23}Na- and ^{1}H-MRI

Three-dimensional transaxial ^{23}Na-MRI images were obtained with a gradient-echo imaging sequence using the following imaging parameters: ~130-μs nonselective excitation radio frequency (RF) pulse, 50-ms repetition time (TR), 4.5-ms echo time (TE), and 64 × 64 × 16 data points over a 60 × 60 × 60-mm field-of view (FOV). A relatively long TE was used to achieve a short bandwidth (10,000 Hz) and optimize the signal-to-noise ratio (SNR) in the ^{23}Na images. The noise in an image is directly proportional to the square root of the bandwidth; thus, decreasing the bandwidth should increase the image SNR. However, decreasing the bandwidth increases the acquisition time and TE, resulting in signal loss due to T_2^* relaxation. The combination of TE and bandwidth used gave the maximum SNR in ^{23}Na-MRI of the rat kidney. In addition, weighted signal summation (WSS) was employed in the two phase-encoding directions to further improve SNR (3). A maximum of 64 and an average of 9.67 transients were collected per phase-encoding steps. Typical scan time was ~10 min. The time domain data were zero-filled once in both phase-encoding directions, giving a 128 × 128 × 16 data matrix, and Fourier-transformed. The processed ^{23}Na-MRI had a 469-μm in-plane resolution and 3.75-mm slice thickness.

Multislice T_2-weighted ^{1}H-MRI was collected using a spin-echo sequence and the following imaging parameters: 2,000-ms TR, 30-ms TE, 128 × 128 data points over 60 × 60-mm FOV, and 16 slices with 0.5-mm slice thickness. A center-to-center slice separation of 3.75 mm was used so that the ^{1}H-MR image slices matched the ^{23}Na slices. Total data collection time for ^{1}H-MRI was 4 min 16 s. The time domain data were zero-filled once, giving a 256 × 256 data matrix, and Fourier-transformed. Delineation of the kidney boundary, cortex, medulla, and pelvis in the ^{23}Na images was performed using the high-resolution ^{1}H images.

T_1 and T_2 Measurements Using MRI

T_1 and T_2 of renal cortex and medulla were measured by ^{23}Na-MRI in two additional cohort of rats (n = 3 each) using the 50-mm-diameter loop-gap resonator. A three-dimensional gradient-echo imaging sequence with similar imaging parameters as describe above was used. The image matrix size was reduced to 64 × 32 × 8 for both T_1 and T_2 measurements. Five ^{23}Na images with a 4.5-ms TE and 10-, 20-, 50-, 80-, and 120-ms TR were collected for T_1 measurement. The measurement was repeated every ~16 min during normal perfusion, 50-min ischemia, and 50-min reperfusion. For T_2 measurements, the readout gradient was increased by a factor of 10 to allow shorter TE, and 10 ^{23}Na images were collected with a 50-ms TR and 1.5-, 2.2-, 3.5-, 4.5-, 6-, 8-, 11-, 15-, 19-, and 25-ms TE. T_2 measurements were repeated every ~25 min during normal perfusion, 50-min ischemia, and 50-min reperfusion.

T_1 and T_2 Measurements Using MRS

The effect of ischemia and reperfusion on ^{23}Na fast and slow T_2 (T_{2f} and T_{2s}, respectively) and T_1 of the whole kidney was evaluated by MRS using a separate cohort of rats (n = 4). The left kidney was exposed through a lateral incision, and the snare taut was placed around the blood vessels. A 10 × 5-mm oval-shaped surface coil tuned to 106 MHz was directly placed on the exposed kidney. ^{23}Na T_1 was measured using a pulse-burst saturation recovery pulse sequence (2) consisting of 10 saturation pulses followed by an incremental delay (16 values ranging from 0.05 to 200 ms), a nominal 90° observe pulse, and acquisition with Cyclops phase cycling. ^{23}Na T_{2f} and T_{2s} were measured using a Hahn spin-echo sequence consisting of a composite 180° pulse. The TE was varied from 0.6 to 40 ms in 16 steps. The instrument dead time of 10 μs was included as a part of the TE. Pairs of T_1 and T_2 data were collected every 16–17 min during normal perfusion, 50-min ischemia, and 50-min reperfusion.

B_1 Homogeneity

Tests on B_1 homogeneity of the slotted-tube resonator used for ^{23}Na-MRI were performed using a cylindrical phantom (height = 75 mm, diameter = 48 mm) filled with 0.3% NaCl solution. Three-dimensional ^{23}Na-MRI images of the phantom were collected using the same imaging parameters as used for the in vivo experiments. The images were processed with Matlab software to analyze the changes in the signal intensity due to B_1 inhomogeneities. A region of interest (ROI) covering both the kidneys and another ROI over the noise region in four middle slices were drawn, and the mean and SD over the ROIs was calculated. The SD in SI for the kidney and noise regions were 2.0 and 2.2%, respectively, relative to the mean of kidney ROI. Thus the RF field produced by the loop-gap resonator was very homogeneous and did not affect quantification of ^{23}Na SI.

Histology

Following the ^{23}Na-MRI experiment, animals were killed by an overdose of anesthesia (5% of isoflurane, 5 l/min). Tissue fixation was achieved by vascular perfusion through the left ventricle with 30 ml of saline followed by 50 ml of 25% zinc-formalin solution (Anathech, Battle Creek, MI). Both kidneys were excised, immersed in formalin overnight, and embedded in paraffin. Histological sections including cortex and medulla were obtained at 3-μm thickness. Sections were stained with hematoxylin and eosin to evaluate cellular detail and periodic acid-Schiff (PAS) to highlight the apical brush borders of proximal tubules. A renal pathologist (C. L. Phillips) scored deidentified slides on an Olympus BX41 brightfield microscope (Olympus) using the methods of Jablonski (20) and Kelly (22, 23).

Data Analysis and Statistics

ROIs on the renal cortex, medulla, and the reference saline tube were drawn on the ^{1}H images using Image Browser software (Varian) and applied to ^{23}Na images. Special care was taken to exclude the renal pelvis from the medulla ROI as shown in Fig. 1. The average ^{23}Na SI relative to the reference was measured for the cortex and medulla ROIs. The ratio of medulla to cortex ^{23}Na SI gave the corticomedullary sodium contrast of the kidney. All relaxation time measurement data were analyzed using PSI-Plot version 4.0 for Windows (Poly Software, Salt Lake City, UT). T_1 of the cortex and medulla was computed from the ^{23}Na-MRI data by least-square fitting the average SI (A) vs. TR plots to the equation

$$A = (A_0 - A_\infty) \times e^{-TR/T_1} + A_\infty, \quad (1)$$

where A_0 and A_∞ are ^{23}Na-MRI SI at TR = 0 and ∞, respectively. The values of A_0, A_∞, and TR were allowed to vary during curve-fitting. Fast and slow T_2 (T_{2f} and T_{2s}, respectively) and the relative fraction of the fast T_2 (f_f) were computed by least-square fitting the average cortex or medulla SI vs. TE plots to the biexponential equation

$$A = A_0 \times \lfloor f_f \times e^{-TE/T_{2f}} + (1 - f_f) \times e^{-TE/T_{2s}} \rfloor, \quad (2)$$

where A_0 is SI at TE = 0. The values of A_0, f_f, T_{2f} and T_{2s} were allowed to vary. Curve fitting of the T_2 image data to *Eq. 2* did not give a reproducible value for T_{2f} because the shortest TE value was 1.5 ms. Thus T_{2f}, T_{2s} and f_f for the whole kidney were calculated by ^{23}Na-MRS by fitting a plot of ^{23}Na resonance areas vs. TE to *Eq. 2*. T_1 for the whole kidney from the MRS data was also evaluated by curve fitting to *Eq. 1*.

TSC in the medulla and cortex were calculated by applying T_1 and T_2 corrections, according to the formula (9, 10, 25, 37)

$$TSC = \frac{A^{tiss} \times [Na]^{std}}{A^{std}} \times \frac{1 - e^{-TR/T_1^{std}}}{1 - e^{-TR/T_1^{tiss}}} \times \frac{e^{-TE/T_2^{std}}}{f_f \times e^{-TE/T_{2f}^{tiss}} + (1 - f_f) \times e^{-TE/T_{2s}^{tiss}}} \quad (3)$$

where, A^{std} and A^{tiss} are the standard saline reference and the tissue SI, respectively. The relaxation times of the standard saline reference containing 51.3 mM NaCl were T_1^{std} = 64 ms, T_2^{std} = 60 ms.

All data are presented as means ± SE. A two-tailed unpaired Student's t-test was used for the comparison of baseline and IR-injured kidney. A P value ≤0.05 was used to define statistical significance.

RESULTS

A selected transaxial section from multislice ^{1}H-MRI of the abdominal region of the rat is shown in Fig. 1*A*. The two kidneys with their subregions and some blood vessels are clearly distinguishable. The ^{1}H images helped in delineating the cortical and medullary regions of the kidney. Figure 1*B* shows a zoomed-in ^{1}H image of the left kidney and ROIs for the renal cortex and medulla that were transferred to ^{23}Na-MRI

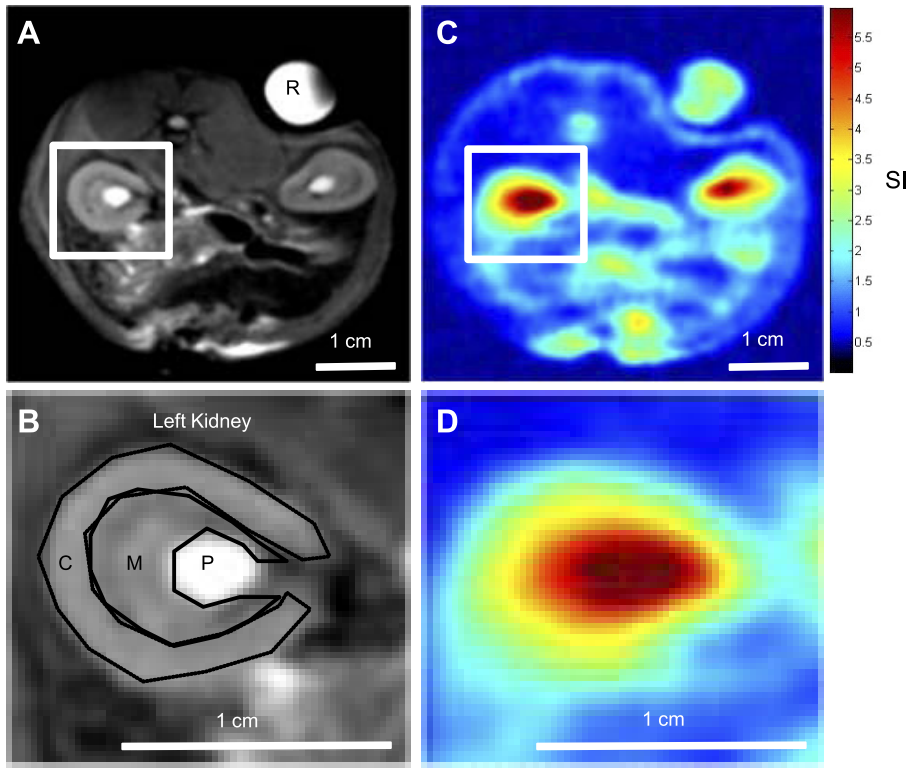

Fig. 1. ^{1}H- and ^{23}Na-magnetic resonance imagery (MRI) of the rat kidney. *A*: transaxial ^{1}H-MRI section through the kidneys. *B*: enlarged ^{1}H-MRI showing the left kidney and regions of interest for the cortex and medulla that were transferred to ^{23}Na-MRI for average signal intensity (SI) measurements. *C*: transaxial section of a 3-dimensional ^{23}Na-MRI corresponding to the ^{1}H-MRI represented in *A*. *D*: enlarged ^{23}Na-MRI of the left kidney. R, reference; C, cortex; M, medulla; P, pelvis. Bar = 1 cm.

for average SI measurements. Figure 1*C* shows the transaxial section from the three-dimensional ^{23}Na-MRI corresponding to the ^{1}H-MRI shown in Fig. 1*A*. Zoomed-in ^{23}Na-MRI of the control rat's left kidney is shown in Fig. 1*D*. The image shows a gradual increase in ^{23}Na SI along the corticomedullary axis from the edge of the cortex through the outer and inner medulla.

The average medullary and cortical ^{23}Na SI with respect to the reference and the medulla-to-cortex ^{23}Na SI ratio for the control rats (0-min ischemia) are shown in the Fig. 2. ^{23}Na SI was similar in both right and left kidney for the cortex (1.67 ± 0.17) and medulla (1.06 ± 0.11). The corticomedullary sodium contrast was found to be ~ 1.61 ± 0.02 in both the kidneys. There was no change in the medullary and cortical ^{23}Na SI (and the corticomedullary sodium contrast) over 2 h in both kidneys of the control rats.

Ischemia and reperfusion injury was applied to the left kidney while the right kidney served as a control. Figure 3 shows representative zoomed-in ^{23}Na-MRI of the left kidney

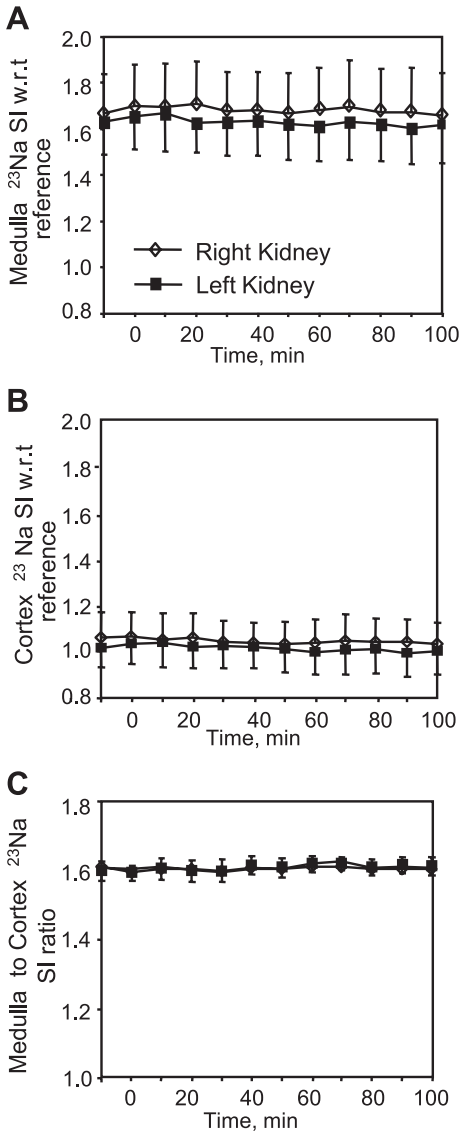

Fig. 2. Profile of the average ^{23}Na SI from the medulla (*A*), cortex (*B*), and medulla-to-cortex ratio (*C*) in the control kidney. Values are means ± SE; $n = 5$.

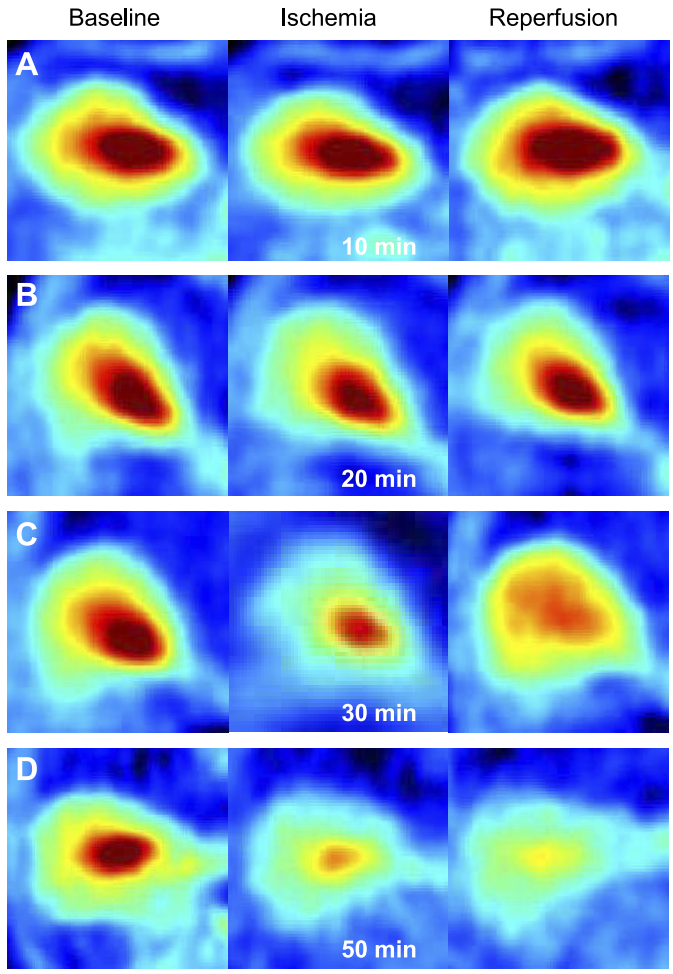

Fig. 3. Enlarged ^{23}Na-MRI of the left kidney collected during baseline, the last 10 min of ischemia, and the last 10 min of reperfusion for 10- (*A*), 20- (*B*), 30- (*C*), and 50-min (*D*) ischemia. Duration of reperfusion was 60 min.

collected during baseline, the last 10 min of ischemia, and the last 10 min of reperfusion for the 10-, 20-, 30-, and 50-min ischemia groups. Changes in the renal sodium distribution during ischemia and reperfusion can be clearly seen, especially in the 30- and 50-min ischemic kidneys. The images reveal larger decreases in ^{23}Na SI from the cortex and medulla with longer ischemic periods.

The time course of the effects of 10-, 20-, 30-, and 50-min ischemia followed by 60-min reperfusion on the average medullary and cortical ^{23}Na SI and the medulla-to-cortex ^{23}Na SI ratio is shown in Fig. 4. After 10 min of ischemia, the medullary ^{23}Na SI decreased by ~14% (from 1.55 ± 0.07 to 1.36 ± 0.12, $P < 0.05$) and the cortical ^{23}Na SI decreased by ~10% (from 0.941 ± 0.04 to 0.86 ± 0.06, $P < 0.05$). ^{23}Na SI in both medulla and cortex recovered after reperfusion. There was no significant change in the corticomedullary sodium contrast during 10 min of ischemia and reperfusion. After 20 min of ischemia, the medullary ^{23}Na SI decreased by ~16% (from 1.6 ± 0.01 to 1.34 ± 0.08, $P \leq 0.05$) and the cortex ^{23}Na SI decreased by ~14% (from 1.01 ± 0.04 to 0.08 ± 0.05, $P >$ 0.05). There was a partial recovery in the medulla ^{23}Na SI but a full recovery in the cortex ^{23}Na SI after 60 min of reperfusion. After 20 min of ischemia, corticomedullary sodium con-

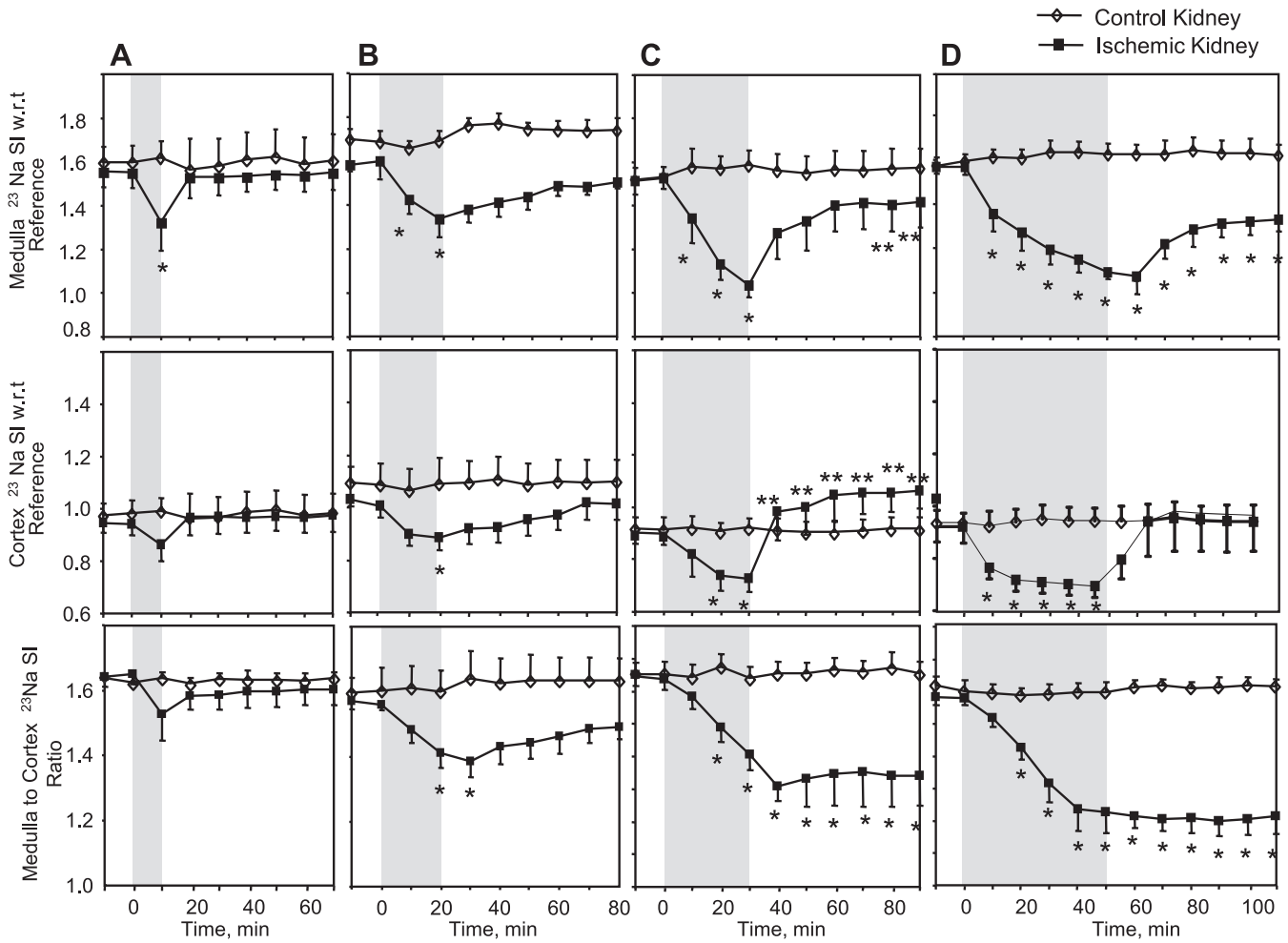

Fig. 4. Effect of 10- (*A*), 20- (*B*), 30- (*C*) and 50-min (*D*) ischemia and reperfusion on ^{23}Na SI from the medulla, cortex and medulla-to-cortex ^{23}Na SI ratio. Shading indicates ischemia period. Values are means ± SE; $n = 5$. *$P < 0.05$ vs. right kidney. **$P < 0.05$ vs. ischemia.

trast decreased by ~10% (from 1.57 ± 0.03 to 1.41 ± 0.05, $P < 0.05$), but it recovered after 50 min of reperfusion. After 30 min of ischemia, the medulla and cortex ^{23}Na SI decreased by ~30% (from 1.53 ± 0.05 to 1.03 ± 0.05, $P < 0.01$) and ~20% (from 0.9 ± 0.04 to 0.73 ± 0.04, $P < 0.05$), respectively. The medulla ^{23}Na SI recovered at 90% of the baseline value during reperfusion but the cortex ^{23}Na SI overshot the baseline level. Corticomedullary sodium contrast decreased by ~15% (from 1.65 ± 0.03 to 1.41 ± 0.05, $P < 0.01$) after 30 min of ischemia. The ratio continued to decrease on reperfusion and plateaued at 1.34 ± 0.1. After 50 min of ischemia, medulla and cortex ^{23}Na SI decreased by ~32% (from 1.57 ± 0.03 to 1.09 ± 0.03, $P < 0.01$) and ~20% (from 0.92 ± 0.06 to 0.74 ± 0.04, $P < 0.01$), respectively. Corticomedullary sodium contrast was decreased by ~25% (from 1.59 ± 0.02 to 1.23 ± 0.06, $P < 0.01$); on reperfusion the ratio continued to decrease and plateaued at 1.21 ± 0.05.

Figure 5 shows effects of ischemia on ^{23}Na T_1 of renal medulla and cortex measured by in vivo ^{23}Na-MRI. Before ischemia, the T_1 of the medulla (35.4 ± 2.4 ms) and cortex (36 ± 2 ms) were similar. Ischemia caused similar decreases in T_1 in both kidney compartments. After 50 min of ischemia, the T_1 of medulla and cortex were 29 ± 3 and 30 ± 3 ms, respectively. The T_1 of both kidney compartments recovered slightly after 50 min of reperfusion. Results of in vivo ^{23}Na-MRS experiments showed similar changes in T_1 of the whole kidney during ischemia and reperfusion (data not shown).

Preliminary analysis of ^{23}Na-MRI data showed monoexponential T_2 because the minimum TE used in the imaging experiment was relatively long (1.5 ms). The failure to detect two T_2 components in the ^{23}Na signal does not exclude the possibility that both fast and slow components are indeed present. An example of curve fitting of typical relaxation time data to mono- and biexponential functions has been added to Fig. 6*A*. T_2 measurements of the whole kidney by ^{23}Na-MRS showed a biexponential T_2 decay. Before ischemia, T_{2s} and T_{2f} of the kidney were 28.4 ± 0.6 and 3.2 ± 0.1 ms, respectively. Both T_{2s} and T_{2f} of the whole kidney decreased to 22 ± 2 and 1.9 ± 0.1 ms, respectively, after 50 min of ischemia. Both the relaxation times recovered slightly after 50 min of reperfusion. Changes in T_{2f} and f_f of the whole kidney during 50-min ischemia and reperfusion are shown in Fig. 6, *B* and *C*, respectively. The relative contribution of the fast and slow relaxation components was 25:75 (fast:slow) before ischemia, 33:67 after 50 min of ischemia, and 34:66 after reperfusion.

Changes in regional ^{23}Na T_{2s} calculated from MRI data using the T_{2f} and f_f from the MRS experiments, are shown in Fig. 7. Before ischemia, T_{2s} of the cortex and medulla were

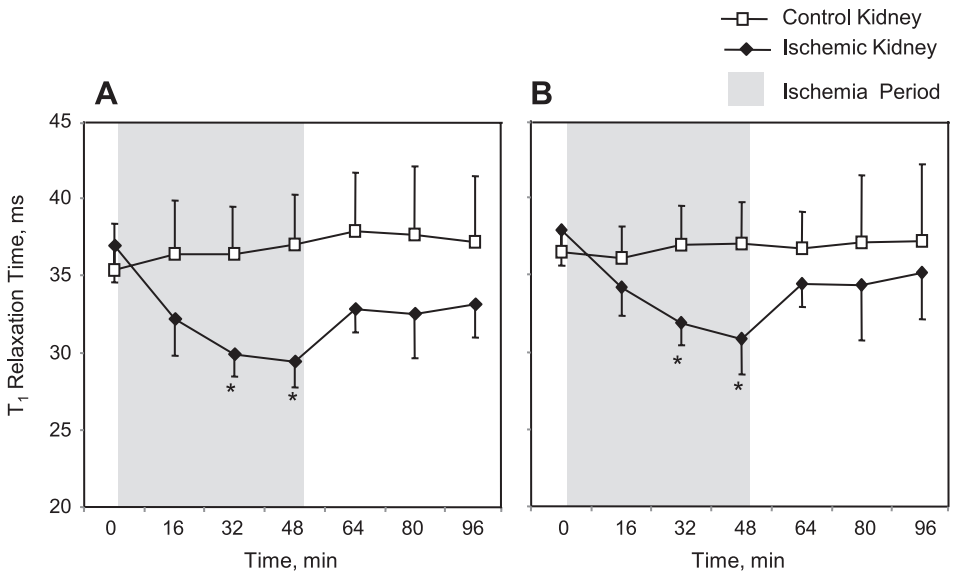

Fig. 5. Effect of ischemia on ^{23}Na relaxation time (T_1) of the medulla (*A*) and cortex (*B*) measured by ^{23}Na-MRI. TE, echo time. Values are means ± SE; $n = 5$. *$P < 0.05$ vs. right kidney.

19 ± 1 and 18 ± 1 ms, respectively. These relaxation times are shorter than the T_2 of the whole kidney measured by MRS because of B_o inhomogeneity effects. The B_0 inhomogeneity factor, $\gamma\Delta B_0$, was estimated to be ~17 s from the T_{2s} values from the MRS and MRI experiments. This B_0 inhomogeneity decreased the T_{2f} to 3.0 ms in MRI experiments compared with 3.2 ms in MRS experiments. Thus the T_{2f} from the MRS experiment value can be used to estimate the regional T_{2s} in the MRI experiments. The T_{2s} of both the medulla and cortex decreased to 13 ± 1 ms after 50 min of ischemia and then increased to 15 ± 1 ms after 50 min of reperfusion.

Figure 8 shows changes in average TSC in the medulla and cortex for the 50-min ischemia-reperfusion experiments. TSC was calculated from the ^{23}Na SI and relaxation times using *Eq. 1* for each time point during baseline, 50-min ischemia, and 60-min reperfusion periods. Ischemia decreased the average TSC from 84.4 ± 3.1 to 70 ± 2.9 mmol/l in the medulla (a 17% decrease) and from 54.3 ± 3.1 to 45.5 ± 2.6 mmol/l in the cortex (a 16% decrease). Although the relative decrease in Na^+ concentration was similar in the medulla (17%) and cortex (16%), it did not recover completely in the medulla but recovered in the cortex after 50 min of reperfusion. Ischemia caused significant changes in ^{23}Na T_1, T_{2s}^*, T_{2f}, and f_f which affected the medulla and cortex TSC. Without correcting for these relaxation time changes, ^{23}Na SI overestimated the decrease in TSC during ischemia by ~15% in both the cortex and the medulla. However, the changes in relaxation times for the medulla and cortex were identical, thus the medulla-to-cortex ^{23}Na SI ratio represents the TSC ratio in the two compartments during ischemia and reperfusion.

Figure 9 shows representative histological sections from a control kidney and from 10, 30 and 50 min ischemic kidneys. The control kidney section shows intact apical brush borders in S3 segments of proximal tubules. In contrast the 50 min ischemia kidney section from superficial renal cortex shows cellular casts in tubule lumina (epithelial cell debris) and disruption of apical brush borders of proximal tubules providing clear evidence of acute tubular damage. According to the Jabolinski method, which includes criteria focusing on renal cortical injury (19, 20), the 10 min ischemia group showed predominantly grades 0 to 1, including minor mitosis and necrosis of individual cells in the cortical proximal tubules. Most of the 20 min ischemia group sections also showed individual cell necrosis and mitosis (grade 1) but some of the sections showed necrosis of all cells in adjacent PCT, with survival of surrounding tubules consistent with Jablonski grade 2. Sections from 30 min ischemia group showed damage consistent with Jablonski grades 2 to 4. 50 min ischemia group sections showed necrosis affecting all three segments of the PT (full thickness cortex) consistent with Jablonski grade 4. According to Kelly histology scaling (22, 23), which addresses injury in outer medulla, i.e., percent of tubules in outer medulla with epithelial cell necrosis or had necrotic debris, the 10 min ischemia group showed no injury, 20 min ischemia group showed 10–25% injury, 30 min ischemia group showed 26–75% injury, and 50 min ischemia group showed greater than 75% injury.

DISCUSSION

Previous studies have shown that proximal tubules (especially the S3 segment) (13, 38) and the outer medullary TAL suffer the most severe injury after an ischemic insult. The proximal tubule is the site of reabsorption of approximately two-thirds of the NaCl that enters the tubular fluid by glomerular filtration. The loop of Henle generates a high osmolality in renal medulla via the countercurrent multiplier, which is dependent on the Na^+ reabsorption by the TAL (39). Several sodium transporters are responsible for this. The apically expressed Na^+-K^+-$2Cl^-$ cotransporter, Na^+/H^+ exchanger, and the basolateral expression of Na^+-K^+-ATPase are key components responsible for sodium reabsorption by the TAL (12, 43). The loss of urinary concentration capacity reflects an altered countercurrent system and is an early indicator of ATN (6, 27). Noninvasive monitoring of the corticomedullary sodium gradient may, therefore, serve as an early real-time indicator of evolving ATN. Herein, we show that the ^{23}Na-MRI revealed a marked change in the ^{23}Na-MRI SI profile of the medulla and cortex and its ratio during ischemia-reperfusion injury. In addition to a change in sodium content, ischemia

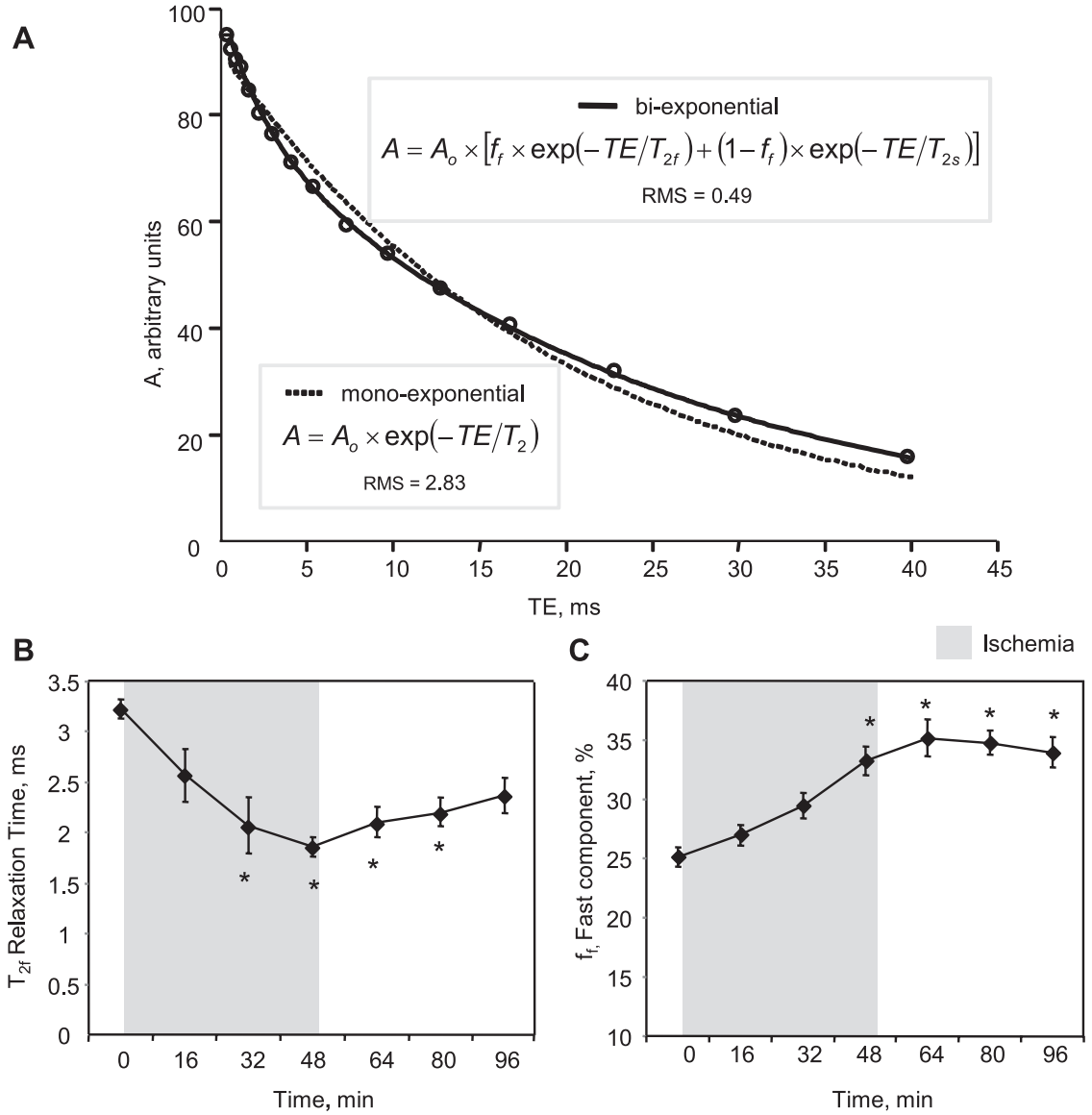

Fig. 6. *A*: example of curve fitting of typical T_2 relaxation time data to mono- and biexponential functions. Effects are shown of ischemia and reperfusion on ^{23}Na fast T_2 (T_{2f}; *B*) and fast T_2 component fraction (f_f; *C*), observed by MRS using a Hahn SE sequence consisting of a composite 180° pulse. These values were computed by fitting a plot ^{23}Na resonance area vs. TE to a biexponential function using a PSI plot. RMS, root mean square deviation. Values are means ± SE; $n = 5$. *$P < 0.05$ vs. control kidney.

and reperfusion can alter ^{23}Na relaxation times, affecting ^{23}Na-MRI SI (4). Hence, the effects of renal ischemia and reperfusion on ^{23}Na relaxation times in the renal medulla and cortex were evaluated, and the changes in TSC due to IR injury were quantified by applying T_1 and T_2 corrections.

Several approaches were used to improve the quality of ^{23}Na-MRI to measure the corticomedullary sodium gradient in the rat kidney. First, a loop-gap resonator tunable to both ^{23}Na and ^{1}H frequencies was used. This coil is relatively simple to build, provides good SNR, has relatively high RF homogeneity, and allows collection of both ^{23}Na- and ^{1}H-MRI for simple coregistration. Second, an optimum combination of TE and bandwidth that provides the highest SNR considering the biexponential T_2 of ^{23}Na was used. Use of 4.5-ms TE resulted in significant loss of the fast T_2 component of the ^{23}Na signal from the kidney, which could have been avoided by using a 1-ms or shorter TE. However, the images with a longer TE had a larger contribution from extracellular Na^+ because T_2 of extracellular Na^+ is mostly monoexponential whereas T_2 of intracellular Na^+ is mostly biexponential. ^{23}Na images with more extracellular Na^+ weighting are more suitable for monitoring the corticomedullary sodium gradient because the gradient is present in the extracellular space. Third, the WSS technique was used to further improve SNR in ^{23}Na-MRI. In this technique, maximum signal transients are collected when the phase-encoding gradient amplitude is minimal and the number of signal transients is reduced as the gradient amplitude increases. The signal transients summed at different phase-encoding steps are varied such that WSS produces similar signal conditioning effects as apodization with a Gaussian function. Data collection with WSS increases the SNR by ~50% compared with apodization after data collection (3).

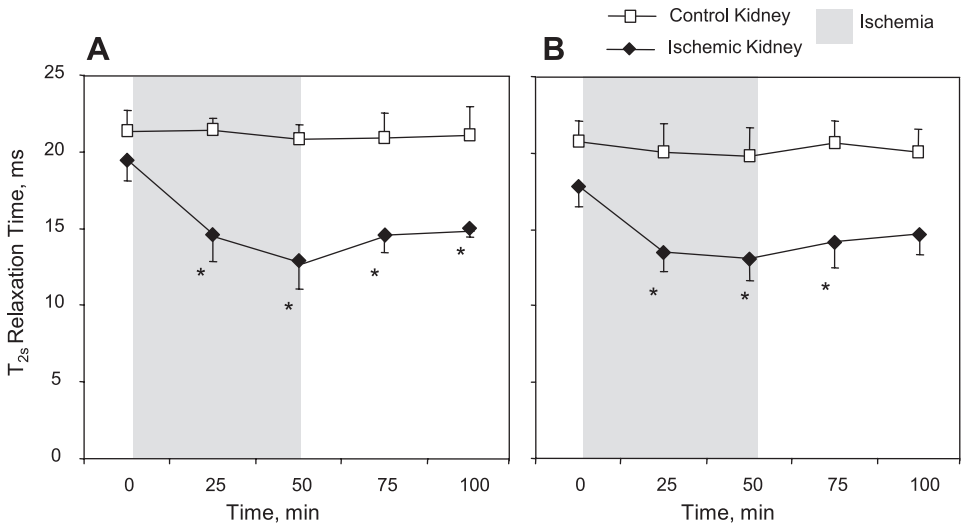

Fig. 7. Effect of ischemia on ^{23}Na T_{2s} of the medulla (*A*) and cortex (*B*) measured by ^{23}Na-MRI. Values are means ± SE; $n = 5$. *$P < 0.05$ vs. right kidney.

This is because in conventional apodization, both signal and noise are multiplied by the weighting function, but with WSS, the signal is multiplied by the weighting function, while the noise is multiplied by the square-root of the weighting function.

Similar to the previous ^{23}Na-MRI studies on rats (24–27, 41), our data show that in the normal kidney ^{23}Na SI increases along the corticomedullary axis. The ratio of ^{23}Na SI in the inner medulla relative to the cortex edge was ~5:1 (ranging from ~1.6 at the tip of the cortex to ~6.5 at the end of the medulla), and the average ^{23}Na SI in the medullary region was ~60% higher than in the cortex. Previous studies by Maril et al. (25) quantified the corticomedullary sodium gradient from the slop of a plot between ^{23}Na SI (normalized to 1 in the start of the cortex) and the distance from cortex along a straight line from the tip of the cortex to the end of the medulla. This analysis yielded a slope of 0.45 ± 0.07 relative SI/mm for the normal kidney, which is in agreement with the previously reported value of 0.51 relative SI/mm (25). The slope analysis gives information about the nature of spatial behavior of the sodium gradient along the corticomedullary axis in a given orientation, but the gradient may vary with different orientations. In addition, the analysis uses data from only a few voxels in the image introducing significant variations in the slope due to random errors. Therefore, the ROI analysis described in MATERIALS AND METHODS was used to serve as a straightforward, fast analytic tool for sodium gradient measurements in the present study.

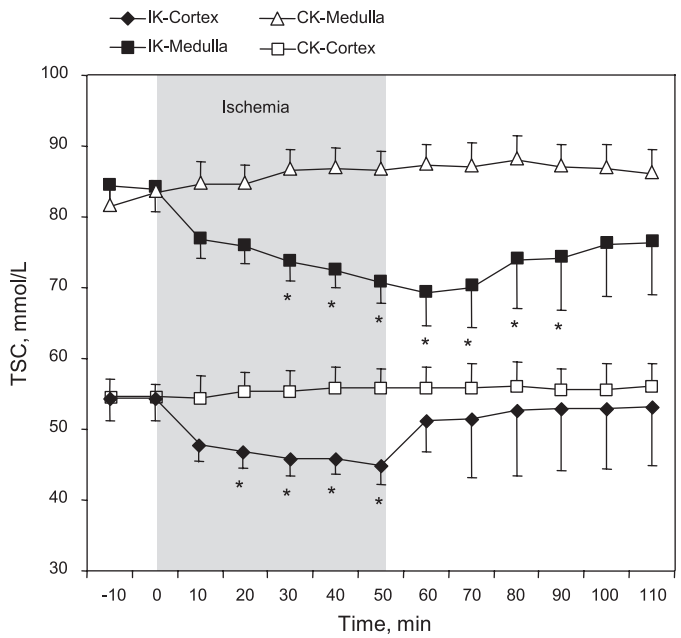

Fig. 8. Effect of 50-min ischemia and 60-min reperfusion on tissue sodium concentration (TSC) in the cortex and medulla of ischemic kidneys (IK) and control kidneys (CK). Values are means ± SE; $n = 5$. *$P < 0.05$ vs. right kidney.

In-magnet IR injury was induced for 10, 20, 30, or 50 min by renal vessel occlusion, and the changes in the sodium gradient were monitored. Ischemic ATN results when hypoperfusion overwhelms the kidney's autoregulatory defenses. Under these conditions, hypoperfusion initiates cell injury that often, but not always, leads to cell death (6). The severity of cellular injury depends on the extent and duration of blood flow reduction (15). Injury of tubular cells is most prominent in the straight portion of the proximal tubules and in the TAL of the loop of Henle, especially as it dips into the relatively hypoxic medulla. It has been suggested that during ischemic injury the proximal tubule Na^+-K^+-ATPase is partly redistributed to the apical plasma membrane in this segment, and its expression may be disregulated, which plays a role in the impaired proximal tubular sodium reabsorption in postischemic kidneys (7, 12–14, 16, 17, 29, 30, 38). Injury to the tubular cells in the TAL also induces reduced tubular reabsorption of Na^+ (42). This reduction in sodium reabsorption is responsible for a decreased sodium gradient across the corticomedullary region. In this study, sodium images clearly demonstrated slight decrease in the medulla-to-cortex sodium gradient after 20 min of ischemia but a much larger decrease after 30 and 50 min of ischemia. The Na^+ gradient recovered completely with 60 min of reperfusion after 10 and 20 min of ischemia, as there was not much damage to the cells and the functional activity is regained after reperfusion. A 30-min or longer ischemia produced an irreversible decrease in the Na^+ gradient.

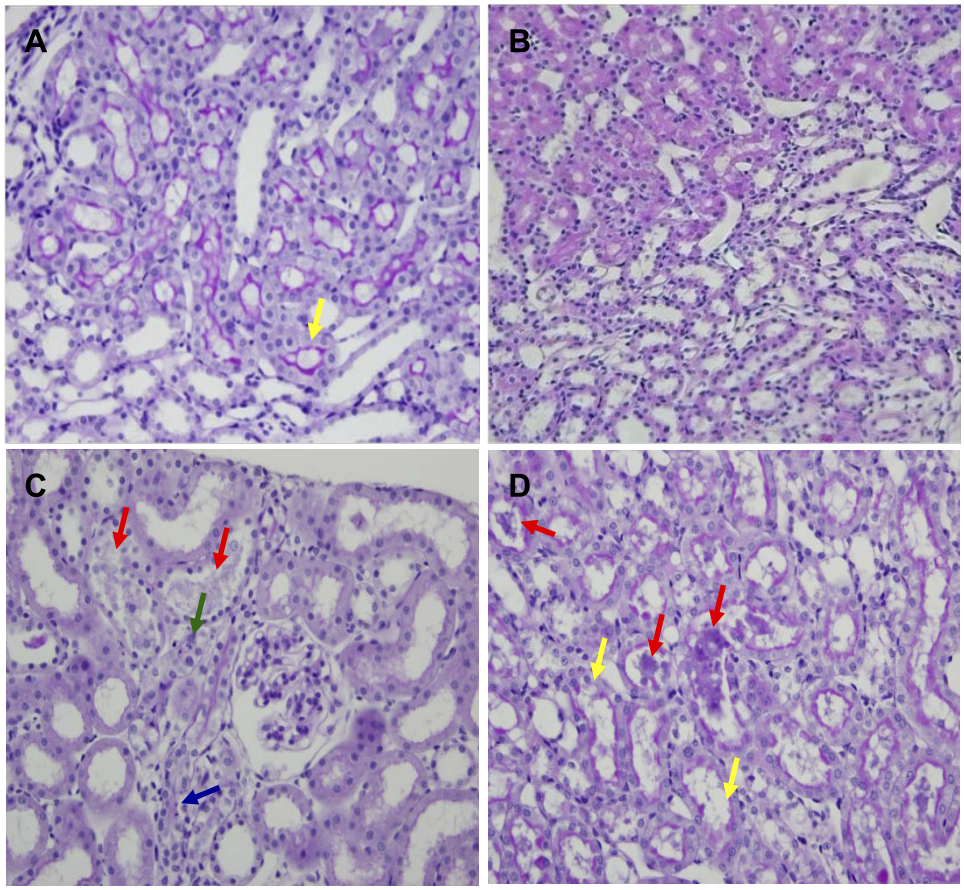

Fig. 9. Histology sections of rat kidneys. *A*: control rat kidney shows intact apical brush borders in S3 segment of proximal tubules (yellow arrow). *B*: 10-min ischemia group does not show evidences of apoptosis or necrosis. *C*: 30-min ischemia group shows dilated tubule lumina, granular casts (red arrows), apoptotic bodies (green arrow), and mitotic figure (blue arrow). *D*: 50-min ischemia group shows cellular casts in tubule lumina (red arrows) and disruption of apical brush borders of proximal tubules (yellow arrows). Magnification ×200 (*A*, *B*, and *D*) and ×400 (*C*). Stain is by periodic acid-Schiff.

The T_1 measured by ^{23}Na-MRI and -MRS showed identical value ~ 37 ms for the normal cortex and medulla. Previous studies have shown similar values of T_1 (25). ^{23}Na exhibits biexponential T_2 relaxation behavior in vivo due to interactions between the electric quadrupole moment of the nucleus and surrounding electronic environment (2, 34). T_{2f} has been reported in the range of 1–3 ms in tissue (2). T_{2f} could not be reliably computed from the MRI experiments in the present study because the shortest TE used was relatively long (1.5 ms). Therefore, the T_{2f} of the exposed kidney was examined by MRS, as it allowed the TE value to be <0.6 ms. T_{2f} was measured to be 3.2 ± 0.1 ms for the exposed kidney before ischemia. The T_1 and T_2 of normal, ischemic, and reperfused kidneys measured by MRI were found to be similar in the cortex and medulla; therefore, it was assumed that the T_{2f} and f_f values measured from the MRS are also similar in the two regions. T_{2s} was calculated from the MRI data using different T_{2f} and f_f values at different time points during baseline, ischemia, and reperfusion.

Renal ischemia and reperfusion caused similar changes in ^{23}Na relaxation times in both the cortex and medulla. T_1, T_{2f}, and T_{2s} all first decreased with ischemia and then increased during reperfusion. The decrease in the relaxation times was most likely due to an increase in intracellular sodium (2, 18), leakage of macromolecules from the intracellular space into the interstitial space (8), and changes in tissue oxygenation level (32). The decrease in ^{23}Na T_1 could also be due to a decrease in temperature during ischemia. All the relaxation times recovered with reperfusion due to extracellular fluid accumulation (8, 18). Other studies have also shown similar trends of a decrease and increase in water ^{1}H T_1 with ischemia and reperfusion (35).

The relative contribution of the fast and slow relaxation components was 25:75 (fast:slow) before ischemia, with a slight increase in the fast-component fraction after ischemia and reperfusion. This ratio is dramatically different from the theoretically expected 60:40 ratio for biexponentially relaxing ^{23}Na in an isotopic sample. Similar deviations from the theoretical ratio have been observed before by Burstein et al. (8) in rat and frog hearts and by Bansal et al. (2) in the rat liver. The observed deviation may be due to the different relaxation characteristics in intra- and extracellular compartments. Intracellular Na^+ is known to have biexponential relaxation due to high macromolecular concentration, whereas extracellular Na^+ is mostly monoexponential. Thus the combination of biexponential and monoexponential Na^+ from intra- and extracellular compartments can give a larger contribution from slow-relaxing Na^+ (1, 2, 4). The changes in T_1 and T_2 with ischemia and reperfusion caused ^{23}Na-MRI SI or visibility to decrease by ~15% for the TE and TR times used in this study.

Relative SI units were converted to TSC units using a sealed saline (0.3% NaCl) tube as a signal reference fixed near the rat's abdomen and taking into account the differences in the T_1 and T_2 relaxation rates between the saline solution and the renal tissue. ^{23}Na T_1 and T_2 relaxation rates in the medulla were same as in the cortex. Hence, the changes in SI in the cortex and medulla regions were directly proportional to changes in TSC. After application of

the T_1 and T_2 corrections, TSC was found to be ~85 mM in the medullary region and ~55 mM in the cortex. A previous study by Bengele et al. (5) using flame photometry reported TSC of 52 mmol/kgH_2O in the cortex and 82 mmol/kgH_2O in the outer medulla, which are similar to the values from ^{23}Na-MRI. TSC was decreased more prominently in the medullary region than in the cortex as there was significant damage in the outer medullary region and to the medullary TAL, which powers the countercurrent mechanism responsible for the hypertonic medullary interstitium. The steep decrease in the TSC during ischemia with no recovery after reperfusion, especially in the 50-min ischemia group, suggests irreversible tubular dysfunction of the kidney.

Histology showed evidence of acute tubular damage that increased with ischemia duration and correlated with the decrease in the corticomedullary sodium gradient during ischemia and reperfusion measured by noninvasive ^{23}Na MRI.

Conclusion

Renal ^{23}Na-MRI revealed a marked change in the corticomedullary sodium gradient during ischemia and reperfusion, which is a major cause of ATN. The inability of the ischemically injured kidney (30 and 50 min of ischemia) to maintain the corticomedullary sodium gradient may indicate irreversible tubular dysfunction of the kidney. ^{23}Na relaxation time measurements by MRI showed that the relaxation characteristics are similar in the renal medulla and cortex in the normal kidney. Ischemia causes a significant decrease in the relaxation times, which affects the calculation of medullary and cortical TSC from MRI SI data. However, the medulla-to-cortex ^{23}Na SI ratio represents the TSC ratio in the two compartments because the changes in relaxation times for the medulla and cortex are identical. Noninvasive renal ^{23}Na-MRI may enable the detection of evolving ATN in the setup of acute renal failure and to differentiate it from other renal diseases where tubular function is maintained. This work can be further extended to clinical studies to diagnose evolving ATN and quantify the severity of injury.

ACKNOWLEDGMENTS

The authors thank J. Larry Solomon for histological staining.

GRANTS

This research was supported in part by National Institutes of Health Grants CA110107 and EB005964.

REFERENCES

1. **Babsky AM, Hekmatyar SK, Zhang H, Solomon JL, Bansal N.** Application of 23Na MRI to monitor chemotherapeutic response in RIF-1 tumors. *Neoplasia* 7: 658–666, 2005.
2. **Bansal N, Germann MJ, Seshan V, Shires GT 3rd, Malloy CR, Sherry AD.** Thulium 1,4,7,10-tetraazacyclododecane-1,4,7,10-tetrakis(methylene phosphonate) as a 23Na shift reagent for the in vivo rat liver. *Biochemistry* 32: 5638–5643, 1993.
3. **Bansal N, Seshan V.** Three-dimensional triple quantum-filtered 23Na imaging of rabbit kidney with weighted signal averaging. *J Magn Reson Imaging* 5: 761–767, 1995.
4. **Bansal N, Szczepaniak L, Ternullo D, Fleckenstein JL, Malloy CR.** Effect of exercise on (23)Na MRI and relaxation characteristics of the human calf muscle. *J Magn Reson Imaging* 11: 532–538, 2000.
5. **Bengele HH, Mathias RS, Perkins JH, Alexander EA.** Urinary concentrating defect in the aged rat. *Am J Physiol Renal Fluid Electrolyte Physiol* 240: F147–F150, 1981.
6. **Brady HR, Singer GG.** Acute renal failure. *Lancet* 346: 1533–1540, 1995.
7. **Brezis M, Rosen S.** Hypoxia of the renal medulla–its implications for disease. *N Engl J Med* 332: 647–655, 1995.
8. **Burstein D, Fossel ET.** Intracellular sodium and lithium NMR relaxation times in the perfused frog heart. *Magn Reson Med* 4: 261–273, 1987.
9. **Christensen JD, Barrere BJ, Boada FE, Vevea JM, Thulborn KR.** Quantitative tissue sodium concentration mapping of normal rat brain. *Magn Reson Med* 36: 83–89, 1996.
10. **Constantinides CD, Kraitchman DL, O'Brien KO, Boada FE, Gillen J, Bottomley PA.** Noninvasive quantification of total sodium concentrations in acute reperfused myocardial infarction using 23Na MRI. *Magn Reson Med* 46: 1144–1151, 2001.
11. **Cross M, Endre ZH, Stewart-Richardson P, Cowin GJ, Westhuyzen J, Duggleby RG, Fleming SJ.** 23Na-NMR detects hypoxic injury in intact kidney: increases in sodium inhibited by DMSO and DMTU. *Magn Reson Med* 30: 465–475, 1993.
12. **Elgavish GA, Elgavish A.** Evidence from 23Na NMR studies for the existence of sodium-channels in the brush border membrane of the renal proximal tubule. *Biochem Biophys Res Commun* 128: 746–753, 1985.
13. **Faarup P, Holstein-Rathlou NH, Norgaard T, Hegedus V.** Early segmental changes in ischemic acute tubular necrosis of the rat kidney. *APMIS* 112: 192–200, 2004.
14. **Fish EM, Molitoris BA.** Alterations in epithelial polarity and the pathogenesis of disease states. *N Engl J Med* 330: 1580–1588, 1994.
15. **Glaumann B, Trump BF.** Studies on the pathogenesis of ischemic cell injury. III. Morphological changes of the proximal pars recta tubules (P3) of the rat kidney made ischemic in vivo. *Virchows Arch B Cell Pathol* 19: 303–323, 1975.
16. **Harvig B, Engberg A, Ericsson JL.** Effects of cold ischemia on the preserved and transplanted rat kidney. Structural changes of the loop of Henle, distal tubule and collecting duct. *Virchows Arch B Cell Pathol Incl Mol Pathol* 34: 173–192, 1980.
17. **Heyman SN, Shina A, Brezis M, Rosen S.** Proximal tubular injury attenuates outer medullary hypoxic damage: studies in perfused rat kidneys. *Exp Nephrol* 10: 259–266, 2002.
18. **Imahashi K, Kusuoka H, Hashimoto K, Yoshioka J, Yamaguchi H, Nishimura T.** Intracellular sodium accumulation during ischemia as the substrate for reperfusion injury. *Circ Res* 84: 1401–1406, 1999.
19. **Jablonski P, Harrison C, Howden B, Rae D, Tavanlis G, Marshall VC, Tange JD.** Cyclosporine and the ischemic rat kidney. *Transplantation* 41: 147–151, 1986.
20. **Jablonski P, Howden BO, Rae DA, Birrell CS, Marshall VC, Tange J.** An experimental model for assessment of renal recovery from warm ischemia. *Transplantation* 35: 198–204, 1983.
21. **Jamison RL.** The renal concentrating mechanism: micropuncture studies of the renal medulla. *Fed Proceedings* 42: 2392–2397, 1983.
22. **Kelly KJ, Tolkoff-Rubin NE, Rubin RH, Williams WW Jr, Meehan SM, Meschter CL, Christenson JG, Bonventre JV.** An oral platelet-activating factor antagonist, Ro-24–4736, protects the rat kidney from ischemic injury. *Am J Physiol Renal Fluid Electrolyte Physiol* 271: F1061–F1067, 1996.
23. **Kelly KJ, Williams WW Jr, Colvin RB, Meehan SM, Springer TA, Gutierrez-Ramos JC, Bonventre JV.** Intercellular adhesion molecule-1-deficient mice are protected against ischemic renal injury. *J Clin Invest* 97: 1056–1063, 1996.
24. **Maeda M, Seo Y, Murakami M, Kuki S, Watari H, Iwasaki S, Uchida H.** Sodium-23 MR imaging of the kidney in guinea pig at 2.1 T, following arterial, venous, and ureteral ligation. *Magn Reson Med* 16: 361–367, 1990.
25. **Maril N, Margalit R, Mispelter J, Degani H.** Functional sodium magnetic resonance imaging of the intact rat kidney. *Kidney Int* 65: 927–935, 2004.
26. **Maril N, Margalit R, Mispelter J, Degani H.** Sodium magnetic resonance imaging of diuresis: spatial and kinetic response. *Magn Reson Med* 53: 545–552, 2005.
27. **Maril N, Margalit R, Rosen S, Heyman SN, Degani H.** Detection of evolving acute tubular necrosis with renal 23Na MRI: studies in rats. *Kidney Int* 69: 765–768, 2006.
28. **Maril N, Rosen Y, Reynolds GH, Ivanishev A, Ngo L, Lenkinski RE.** Sodium MRI of the human kidney at 3 Tesla. *Magn Reson Med* 56: 1229–1234, 2006.

29. **McIntosh BJ, Huang KC.** Effect of renal ischemia on renal tubular function in the rat as measured by PAH uptake in vitro. *Am J Physiol* 182: 124–130, 1955.
30. **Molitoris BA, Wilson PD, Schrier RW, Simon FR.** Ischemia induces partial loss of surface membrane polarity and accumulation of putative calcium ionophores. *J Clin Invest* 76: 2097–2105, 1985.
31. **Ofstad J.** Osmolality in the human kidney. *Scand J Clin Lab Invest* 21: 95–96, 1968.
32. **Prasad PV.** Evaluation of intra-renal oxygenation by BOLD MRI. *Nephron Clin Pract* 103: c58–c65, 2006.
33. **Ra JB, Hilal SK, Oh CH, Mun IK.** In vivo magnetic resonance imaging of sodium in the human body. *Magn Reson Med* 7: 11–22, 1988.
34. **Shinar H, Navon G.** Sodium-23 NMR relaxation times in body fluids. *Magn Reson Med* 3: 927–934, 1986.
35. **Slutsky RA, Andre MP, Mattrey RF, Brahme FJ.** In vitro magnetic relaxation times of the ischemic and reperfused rabbit kidney: concise communication. *J Nucl Med* 25: 38–41, 1984.
36. **Steidle G, Graf H, Schick F.** Sodium 3-D MRI of the human torso using a volume coil. *Magn Reson Imaging* 22: 171–180, 2004.
37. **Thulborn KR, Davis D, Adams H, Gindin T, Zhou J.** Quantitative tissue sodium concentration mapping of the growth of focal cerebral tumors with sodium magnetic resonance imaging. *Magn Reson Med* 41: 351–359, 1999.
38. **Venkatachalam MA, Bernard DB, Donohoe JF, Levinsky NG.** Ischemic damage and repair in the rat proximal tubule: differences among the S1, S2, and S3 segments. *Kidney Int* 14: 31–49, 1978.
39. **Wang X, Thomas SR, Wexler AS.** Outer medullary anatomy and the urine concentrating mechanism. *Am J Physiol Renal Physiol* 274: F413–F424, 1998.
40. **Wang Z, Rabb H, Craig T, Burnham C, Shull GE, Soleimani M.** Ischemic-reperfusion injury in the kidney: overexpression of colonic H^+-K^+-ATPase and suppression of NHE-3. *Kidney Int* 51: 1106–1115, 1997.
41. **Wolff SD, Eng J, Berkowitz BA, James S, Balaban RS.** Sodium-23 nuclear magnetic resonance imaging of the rabbit kidney in vivo. *Am J Physiol Renal Fluid Electrolyte Physiol* 258: F1125–F1131, 1990.
42. **Wu MS, Yang CW, Pan MJ, Chang CT, Chen YC.** Reduced renal Na^+-K^+-Cl^- co-transporter activity and inhibited NKCC2 mRNA expression by *Leptospira shermani*: from bed-side to bench. *Nephrol Dial Transplant* 19: 2472–2479, 2004.
43. **Yamashita J, Ohkita M, Takaoka M, Kaneshiro Y, Matsuo T, Kaneko K, Matsumura Y.** Role of Na^+/H^+ exchanger in the pathogenesis of ischemic acute renal failure in mice. *J Cardiovasc Pharmacol* 49: 154–160, 2007.